Magnetic evidence for a partially differentiated carbonaceous chondrite parent body

Laurent Carporzen[a,1], Benjamin P. Weiss[a,2], Linda T. Elkins-Tanton[a], David L. Shuster[b,c], Denton Ebel[d], and Jérôme Gattacceca[e]

[a]Department of Earth, Atmospheric, and Planetary Sciences, Massachusetts Institute of Technology, Cambridge, MA 02139; [b]Berkeley Geochronology Center, Berkeley, CA 94709; [c]Department of Earth and Planetary Science, University of California, Berkeley, CA 94720; [d]Department of Earth and Planetary Sciences, American Museum of Natural History, New York, NY 10024; and [e]Centre Européen de Recherche et d'Enseignement des Géosciences de l'Environnement, Centre National de la Recherche Scientifique, Université Aix-Marseille 3, F-13545 Aix-en-Provence, France

Edited by David J. Stevenson, California Institute of Technology, Pasadena, CA, and approved February 22, 2011 (received for review November 23, 2010)

The textures of chondritic meteorites demonstrate that they are not the products of planetary melting processes. This has long been interpreted as evidence that chondrite parent bodies never experienced large-scale melting. As a result, the paleomagnetism of the CV carbonaceous chondrite Allende, most of which was acquired after accretion of the parent body, has been a long-standing mystery. The possibility of a core dynamo like that known for achondrite parent bodies has been discounted because chondrite parent bodies are assumed to be undifferentiated. Resolution of this conundrum requires a determination of the age and timescale over which Allende acquired its magnetization. Here, we report that Allende's magnetization was acquired over several million years (Ma) during metasomatism on the parent planetesimal in a $>\sim 20\ \mu$T field up to approximately 9—10 Ma after solar system formation. This field was present too recently and directionally stable for too long to have been generated by the protoplanetary disk or young Sun. The field intensity is in the range expected for planetesimal core dynamos, suggesting that CV chondrites are derived from the outer, unmelted layer of a partially differentiated body with a convecting metallic core.

differentiation | planetesimal | magnetic field | early solar system | paleointensity

Allende is an accretionary breccia from near the surface of the CV parent planetesimal (1). Following accretion, Allende experienced minor aqueous alteration and moderate thermal metamorphism and metasomatism (2) but has remained essentially unshocked (<5 GPa) (3). Its major ferromagnetic minerals are pyrrhotite, magnetite, and awaruite, with an average pseudo single-domain crystal size (4–8). We conducted alternating-field (AF) and thermal demagnetization, rock magnetic, and paleointensity measurements on 71 mutually oriented bulk subsamples of Allende sample AMNH5056 (approximately 10-cm diameter and 8-mm thick slab surrounded by fusion crust). Of these, 51 subsamples were taken from the interior of the meteorite (>1 mm from fusion crust), whereas 20 contained some fusion crust.

The differing magnetization directions of interior and fusion-crusted samples demonstrate that >95% of the natural remanent magnetization (NRM) in interior samples is preterrestrial (Figs. 1 and 2 and *SI Appendix*). AF demagnetization revealed that the interior samples have at least two components: a weak, low-coercivity, nonunidirectional component blocked up to 5 or 10 mT and a high-coercivity (HC) component blocked from approximately 10 to >290 mT (Fig. 1). In agreement with previous studies (4, 9, 10), the HC magnetization is unidirectionally oriented throughout the meteorite's interior (Fig. 2 and *SI Appendix*, Table S1). Thermal demagnetization (Figs. 1 and 2 and *SI Appendix*) indicates that interior samples have a low-temperature (LT) component blocked up to approximately 190 °C, a dominant middle-temperature (MT) component blocked between approximately 190–300 °C and oriented similarly to the HC component isolated by AF demagnetization, and a very weak nonunidirectional high-temperature (HT) magnetization blocked up to approximately 400–600 °C. The MT and LT components are each unidirectional throughout the meteorite and collectively constitute the majority (approximately 90%) of the interior NRM. Similar results were obtained by previous investigators (4, 5, 10). The HC component (Fig. 1) and its association with sulfide-rich separates demonstrates that it is carried predominantly by pyrrhotite (5, 11) (see *SI Appendix*). Blocking temperature relations and our magnetic viscosity experiments indicate that whereas the MT component should have been thermally stable at ambient temperatures over the last 4.5 billion years, the LT component may be a viscous remanent magnetization acquired in a strong (approximately 500 μT) crustal or fine-scale magnetostatic interaction field on the CV parent body (see *SI Appendix*). It is not clear whether the HT remanence is part of the meteorite's NRM or is instead simply an artifact of the laboratory demagnetization process (see *SI Appendix*).

The unidirectionality of the MT component requires that it was acquired following accretion of the CV parent body. This is consistent with the fact that the main NRM carriers (pyrrhotite, magnetite, and awaruite) are thought to be predominantly subsolidus alteration phases produced during hydrous alteration and thermal metamorphism on the parent body (2) (see *SI Appendix*). However, it has previously been unclear exactly how the MT component originated because its upper blocking temperature limit is close to pyrrhotite's ~320 °C Curie point: There have been differing conclusions (4, 10, 11) about whether it is a crystallization remanent magnetization (CRM) from low-temperature sulfidization or a partial thermoremanent magnetization (pTRM) acquired during metasomatism of the parent body. Our high-resolution thermal demagnetization schedule and laboratory TRM experiments strongly favor a 290 °C pTRM (see *SI Appendix*). Additional strong evidence in favor of a pTRM or thermochemical remanence (TCRM) origin is provided by a variety of recently published petrologic constraints that indicate metamorphism to peak temperatures of approximately 250 to <600 °C (see *SI Appendix*), essentially indistinguishable from the peak blocking temperature of the MT component.

Regardless of whether the MT component is a pTRM or TCRM, its unidirectional orientation—now observed by four

---

Author contributions: L.C. and B.P.W. designed research; L.C., L.T.E.-T., D.L.S., D.E., and J.G. performed research; D.L.S. and J.G. contributed new reagents/analytic tools; L.T.E.-T. provided theoretical context; L.C., B.P.W., D.E., and J.G. analyzed data; and L.C., B.P.W., D.L.S., and J.G. wrote the paper.

The authors declare no conflict of interest.

This article is a PNAS Direct Submission.

[1]Present address: Équipe de paléomagnétisme, Institut de Physique du Globe de Paris, Sorbonne Paris Cité, Université Paris Diderot, Centre National de la Recherche Scientifique, F-75005 Paris, France.

[2]To whom correspondence should be addressed. E-mail: bpweiss@mit.edu.

This article contains supporting information online at www.pnas.org/lookup/suppl/doi:10.1073/pnas.1017165108/-/DCSupplemental.

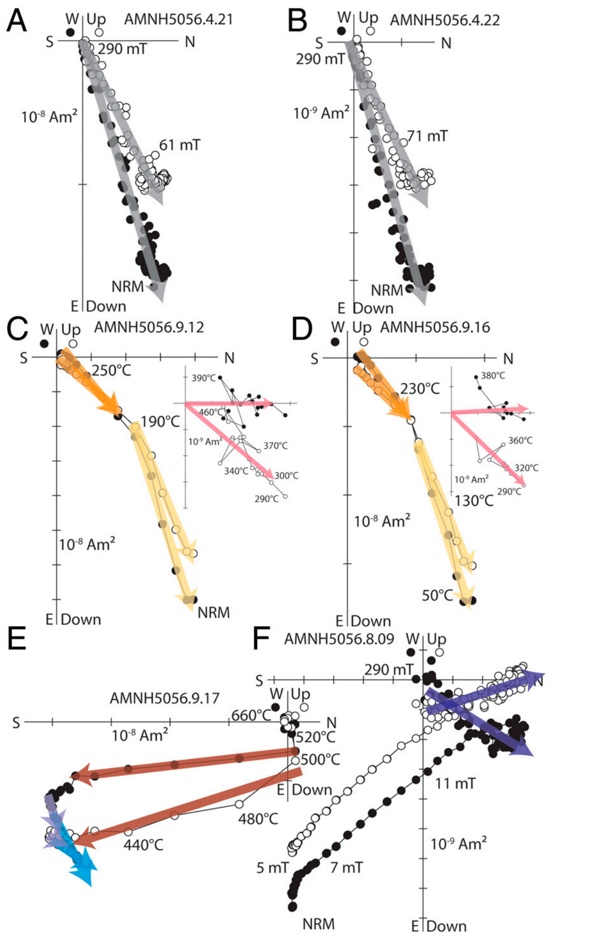

Fig. 1. AF and thermal demagnetization of Allende sample AMNH5056. Shown is a two-dimensional projection of the endpoint of the NRM vector during AF demagnetization. Closed and open symbols represent end points of magnetization projected onto horizontal (N-S-E-W) and vertical (U-D-E-W) planes, respectively. Peak fields for selected AF steps and peak temperatures for selected thermal steps are shown. (*A* and *B*) AF demagnetization of interior subsamples 4.21 and 4.22 reveals a dominantly single-component HC component (gray arrows). (*C* and *D*) Thermal demagnetization of interior subsamples 9.12 and 9.16 confirms that nearly all (>95%) of the remanence is composed of an LT component (blocked up to 190 °C; yellow arrows) and an MT component (blocked from 190–290 °C; orange arrows). *Insets* show the HT demagnetization steps that characterize the scattered HT remanence. (*E*) Thermal demagnetization of fusion-crusted sample 9.17. (*F*) AF demagnetization of fusion-crusted sample 8.09.

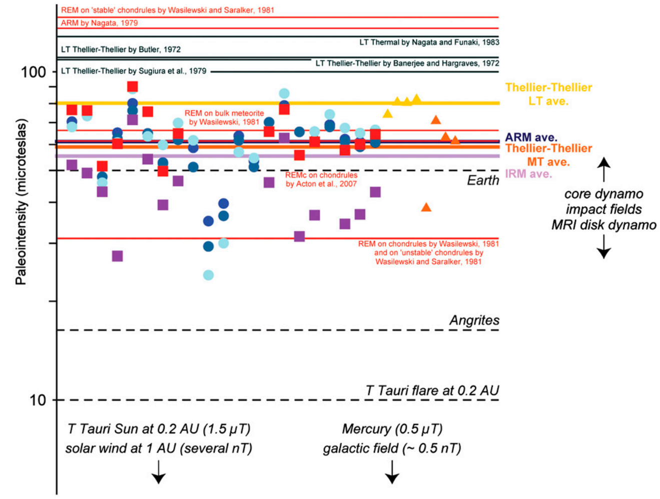

Fig. 3. Summary of paleointensities obtained for Allende. Each vertical cluster of points is derived from a single subsample in our study: circles, thermally calibrated anhysteretic remanent magnetization (ARM) paleointensities; squares, thermally calibrated IRM paleointensities; triangles, Thellier–Thellier paleointensities. Colors correspond to ARM bias fields of 50 μT (light blue), 200 μT (midblue), and 600 μT (dark blue), IRM (red) and REM′ (purple), and LT (yellow) and MT (orange) paleointensities. Mean paleointensities from our ARM and IRM experiments (thermally calibrated from our measurements of ARM/TRM and IRM/TRM) are given by blue and purple lines, respectively. Mean paleointensities from our Thellier–Thellier experiments for the LT and MT components are given by the yellow and orange lines, respectively. For comparison, also shown in solid red and black lines are the mean previously measured paleointensities from Thellier–Thellier and AF (e.g., REM, REMc, ARM) methods, respectively (4–6, 9, 11, 25, 28, 29). REM and REMc are variants of the IRM paleointensity method (see ref. 6). We thermally calibrated the latter paleointensities also using our measurements of TRM/ARM and TRM/IRM. Shown for comparison are the surface fields of the Earth, the solar wind field 1 astronomical unit (AU) from the Sun, the galactic field, the inferred paleofields of a T Tauri short-lived flare at 0.2 AU, and surface fields inferred for the angrite parent body (12).

different laboratories (4, 9, 10)—combined with the lack of significant NRM blocked above 290 °C strongly argues against exotic scenarios like origin in a near-zero background field via magnetostatic interactions (which require preexisting strong NRM to produce such a directionally uniform component). We conducted paleointensity experiments using both Thellier–Thellier and AF-based (12) methods in order to obtain an order-of-magnitude estimate of the paleofields that produced the MT component (see *SI Appendix*). Our results indicate that it formed in fields of order 60 μT with a minimum value of 20 μT (Fig. 3

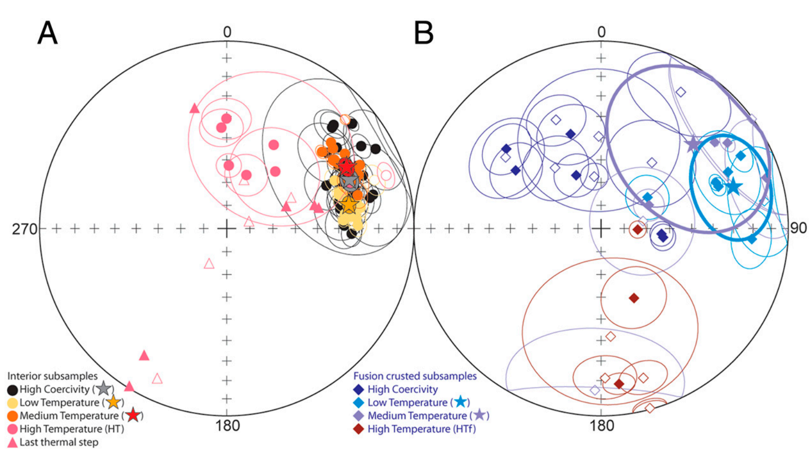

Fig. 2. Equal area plot showing directions of primary magnetization components of Allende subsamples from the interior (circle and triangles) (*A*) and fusion-crusted exterior (diamonds) (*B*). Solid symbols, lower hemisphere; open symbols, upper hemisphere. This plot is oriented in the same way as Fig. 1, with inclination = 90° oriented out of the page (perpendicular to the slab saw cut plane) and declination = 0° oriented toward the top of the page. Sample data ellipsoids are defined as maximum angular deviations associated with the least-squares fits. Stars and their ellipsoids represent the average directions and associated 95% confidence intervals (see *SI Appendix*, Table S1). Samples represented by triangles were only thermally demagnetized to 320 or 330 °C; the directions shown for these samples are the directions at this temperature (rather than a least-squares fit).

and *SI Appendix*). These strong paleointensities stringently constrain the origin and nature of the possible paleofield.

Several different geochronometers constrain the timing and duration of the magnetization acquisition. Pb/Pb (13) and Al/Mg (14) chronometry indicate that chondrules in CV chondrites formed over a period starting possibly within 0.2 Ma of calcium aluminum inclusion (CAI) formation and lasting for somewhere between 1.2–3 Ma (with most chondrules seeming to have formed approximately 1.7 Ma after CAIs) (see *SI Appendix*). Mn/Cr ages of secondary fayalite formed during aqueous alteration of six CV3 chondrites are approximately 5–8 Ma after CAIs (15) (see *SI Appendix*). Because aqueous alteration ended before or coincidentally with thermal metamorphism (16), the MT magnetization in Allende was acquired at or after these times. Most importantly, I/Xe ages of Allende CAIs (17) are younger than I/Xe ages of dark inclusions, refractory inclusions, and chondrules, and up to 9–10 Ma younger than the formation of CAIs (18). Assuming the I/Xe system records thermal disturbances, our I/Xe thermochronological modeling (Fig. 4 and *SI Appendix*, Fig. S13) indicates that elevated thermal conditions (mean temperature of approximately 400 °C) lasted for several Ma ending at approximately 4,559 Ma. Such prolonged heating and cooling is consistent with a variety of other datasets. For example, the compositions of metal, sulfide, and oxide phases in Allende indicate prograde metamorphism at approximately 500 °C for $>10^3$–10^4 y (19).

Because chondrite parent bodies are assumed to be undifferentiated (20–23), the possibility of a core dynamo (24) has been discounted (6, 25–29) in support of early solar system external field sources. These ages indicate that the NRM in Allende is likely too young to have been produced by postulated early external field sources like the T Tauri Sun or the magnetorotational stability in the protoplanetary disk (30). Furthermore, the long (at least several Ma) duration of Allende metamorphism also would make it difficult for such field sources to produce a unidirectional magnetization in the spinning, orbiting CV parent body. Such a long timescale also precludes thermoremanent records of impact-generated fields [which should last <1 d even

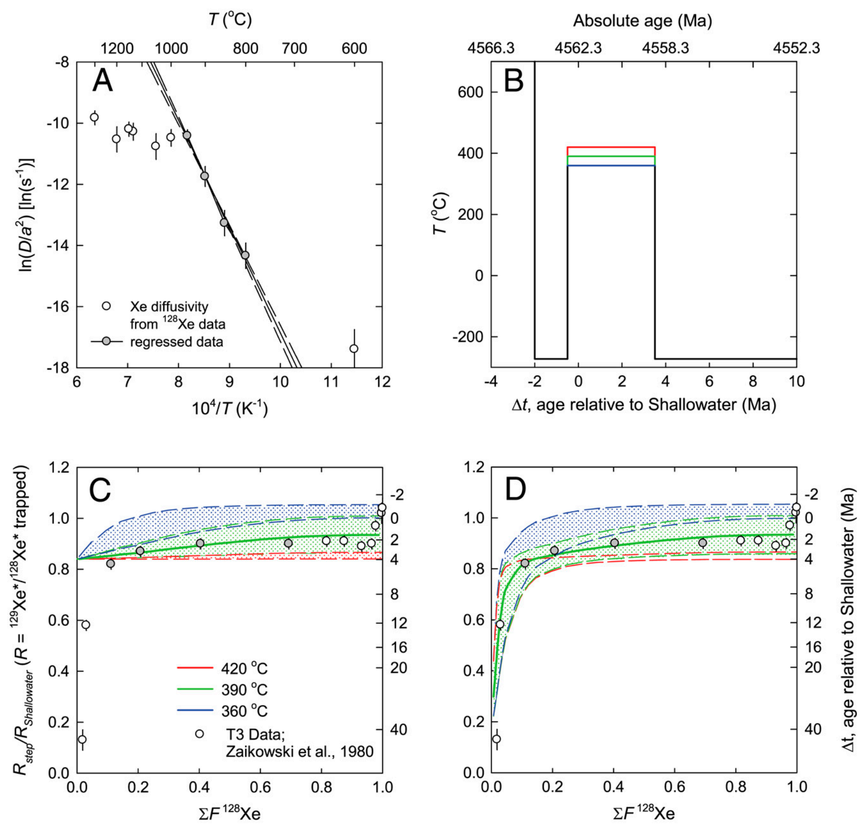

Fig. 4. $^{129}Xe/^{128}Xe$ thermochronology of Allende CAI T3. These calculations use stepped degassing Xe data of ref. 17 (see *SI Appendix*). (*A*) Xe diffusivity as a function of temperature (Arrhenius plot). Points are diffusion coefficients calculated using measured ^{128}Xe release fractions (see *SI Appendix*). The solid line is the model $D(T)/a^2$ obtained from the linear regressions to approximately 50% of the ^{128}Xe data (collected between 800 and 950 °C, indicated by gray points in *A*, *C*, and *D*) and used to calculate the curves shown in *C* and *D*; dashed lines indicate 1σ confidence interval on the regression. This regression corresponds to an activation energy (E_a) for Xe diffusion = 289 ± 16 kJ/mol and a frequency factor $[\ln(D_0/a^2)] = 17.9 \pm 1.7[\ln(s^{-1})]$. $D(T)$ is the diffusivity of Xe as a function of temperature T, and a is the radius of the model diffusion domain. Extractions below 800 °C apparently sampled sites within the CAI with lower Xe retentivity, and the break in slope approximately 950 °C either reflects a phase transition during the analysis or a threshold temperature above which the analysis progressively sampled sites with higher Xe retentivity. (*B*) Simple thermal models tested against the Allende CAI $^{129}Xe^*/^{128}Xe^*$ data shown as temperature (T) plotted as a function of time relative to the I-Xe age of the Shallowater enstatite neutron fluence monitor (see *SI Appendix*). Positive (negative) values indicate time after (before) the I-Xe age of Shallowater. Present time would plot far off scale to the right. (*C* and *D*) Measured and modeled $^{129}Xe^*/^{128}Xe^*$ ratio evolution spectra for the T3 CAI. $^{129}Xe^*/^{128}Xe^*$ represents the radiogenic ^{129}Xe component of each step after subtracting a common ordinary chondrite "OC-Xe" component (see *SI Appendix*). Circles are the $^{129}Xe^*/^{128}Xe^*$ ratios of each step (R_{step}) with associated uncertainties normalized to the ratio of Shallowater ($R_{Shallowater}$) plotted versus the cumulative ^{128}Xe release fraction ($\Sigma F^{128}Xe$). Shown for reference on the right hand *y* axes of each plot are the apparent I-Xe ages of each step calculated relative to Shallowater. Also shown as curves in *C* are modeled release spectra using a spherical, one-domain model for the thermal histories shown in *B*. The curves in *D* are calculated using the same conditions as in *C* but also illustrate the effect of an additional phase with low Xe retentivity. Although the Xe diffusion kinetics for the lower retentivity site(s) is not well quantified (*A*), the young apparent age of the first step (approximately 40 Ma) indicates that the low retentivity sites did not quantitatively retain radiogenic ^{129}Xe until that point in time or after. These calculations indicate that the apparent spatial distribution of radiogenic ^{129}Xe within the Allende T3 CAI is well explained by an approximately 4 Ma long metamorphic event at a mean

for the largest impactors (31)]. Note that even if Allende had an LT (<25 °C) CRM instead of TRM, the timescales of aqueous alteration [estimated to be approximately 1–10^4 y (32)] were likely still too long for recording these external field sources. Finally, the low ratio of NRM to saturation isothermal remanent magnetization (IRM) precludes nebular lightning as a field source.

Allende's paleointensities (Fig. 3) are in the range expected for core dynamos in early planetesimals (12) and other large bodies. Hf/W chronometry indicates that metallic cores formed in planetesimals prior to the final assembly of chondrite parent bodies (33). Recent paleomagnetic analyses of angrites (12) indicate that dynamos were likely generated in convecting metallic cores lasting for ≥11 Ma after solar system formation. Because such bodies melt from the inside out, some may preserve an unmelted, relic chondritic surface that could be magnetized during metasomatism in the presence of a core dynamo. A simple interpretation of Allende's paleomagnetic record is therefore that the CV parent planetesimal is such a partially differentiated object. Therefore, despite widespread practice (e.g., ref. 26), the LT and MT magnetization in Allende cannot be used to constrain the intensity of early protoplanetary disk fields. The HT magnetization might be a preaccretional record of such fields as suggested by ref. 26, but more analyses are required to verify this possibility (see *SI Appendix*).

Planetesimals apparently evolved into a diversity of differentiated end states, from unmelted primitive bodies, to partially molten objects with primitive crusts, to fully melted objects. There should perhaps be extant samples derived from the once-hot interior of the CV parent body: Although oxygen isotope and other geochemical data clearly rule out the hypothesis of a single parent body for all meteorites, they permit the possibility that some chondrite and some achondrite groups originated on a single body. In fact, such samples may already have been discovered. Perhaps metamorphosed CK chondrites (34), coarse-grained clasts in the CV chondrites Mokoia (2) and Y-86009 (35), and/or the metamorphosed chondrite NWA 3133 (36) are samples of the deep crust, wheras the Eagle Station pallasite grouplet (36) and the iron meteorites Bocaiuva and NWA 176 (36) are samples from the melted interior. Further geochemical analyses of these meteorites are required to validate this hypothesis.

Our results suggest that asteroids with differentiated interiors could be present today but masked under chondritic surfaces, which would explain the great discrepancy between the >80% of meteorite parent bodies that melted versus the paucity of asteroids with basaltic surfaces (37). In fact, CV chondrites have spectral signatures similar to many members of the Eos dynamical asteroid family; the spectral diversity of this family has already led to suggestion that the parent asteroid was partially differentiated (38). In any case, the very existence of primitive achondrites, which contain evidence of relict chondrules, metamorphism, and partial melting, are prima facie evidence for the past existence of partially differentiated bodies.

ACKNOWLEDGMENTS. We thank J. Boesenberg and the American Museum of Natural History for providing sample of Allende; L. C. Alexander, S. Bowring, N. Dauphas, M. Funaki, R. Hewins, A. Irving, S. Jacobsen, A. Jambon, E. Lima, D. Mittlefehldt, B. Zanda, Y. Gallet, and M. Zuber for discussions; M. Boustie and L. Berthe for assisting with the laser shock experiments; J. Kirschvink for sharing automated sample handling technology; and K. Willis and B. Carbone for administrative help. B.P.W. thanks the Victor P. Starr Career Development Professorship and the National Aeronautics and Space Administration Origins of Solar Systems Program, and D.L.S. thanks the Ann and Gordon Getty Foundation fund for support.

1. Wood JA (1988) Chondritic meteorites and the solar nebula. *Annu Rev Earth Planet Sci* 16:53–72.
2. Krot AN, et al. (2006) *Meteorites and the Early Solar System II*, eds DS Lauretta and HY McSween (University of Arizona Press, Tucson, AZ), pp 525–553.
3. Scott ERD, Keil K, Stoffler D (1992) Shock metamorphism of carbonaceous chondrites. *Geochim Cosmochim Acta* 56:4281–4293.
4. Nagata T, Funaki M (1983) Paleointensity of the Allende carbonaceous chondrite. *Mem Natl Inst Polar Res Spec Issue* 30:403–434.
5. Wasilewski P (1981) New magnetic results from Allende C3(V). *Phys Earth Planet Inter* 26:134–148.
6. Acton G, et al. (2007) Micromagnetic coercivity distributions and interactions in chondrules with implications for paleointensities of the early solar system. *J Geophys Res* 112, 10.1029/2006JB004655.
7. Flores-Gutiérrez D, Fucugauchi JU (2002) Hysteresis properties of chondritic meteorites: New results for chondrules from the Allende meteorite. *Geofis Int* 41:179–188.
8. Thorpe AN, Senftle FE, Grant JR (2002) Magnetic study of magnetite in the Tagish Lack meteorite. *Meteorit Planet Sci* 37:763–771.
9. Butler RF (1972) Natural remanent magnetization and thermomagnetic properties of Allende meteorite. *Earth Planet Sci Lett* 17:120–128.
10. Sugiura N, Strangway DW (1985) NRM directions around a centimeter-sized dark inclusion in Allende. *Proceedings of the Fifteenth Lunar and Planetary Science Conference* (American Geophysical Union, Washington, DC), pp C729–C738.
11. Wasilewski PJ, Saralker C (1981) Stable NRM and mineralogy in Allende: Chondrules. *Proceedings of the Twelfth Lunar and Planetary Science Conference* (Pergamon, New York), pp 1217–1227.
12. Weiss BP, et al. (2008) Magnetism on the angrite parent body and the early differentiation of planetesimals. *Science* 322:713–716.
13. Connelly JN, Amelin Y, Krot AN, Bizzarro M (2008) Chronology of the solar system's oldest solids. *Astrophys J* 675:L121–L124.
14. Bizzarro M, Baker JA, Haack H (2004) Mg isotope evidence for contemporaneous formation of chondrules and refractory inclusions. *Nature* 431:275–278.
15. Jogo K, Nakamura T, Ito M, Messenger S (2010) Mn-Cr systematics of secondary fayalites in the CV3 carbonaceous chondrites A881317, MET00430 and MET01074. *Lunar Planet Sci* 41 1573.
16. Brearley AJ (1997) Disordered biopyroboles, amphibole, and talc in the Allende meteorite: Products of nebular or parent body aqueous alteration? *Science* 276:1103–1105.
17. Zaikowski A (1980) I-Xe dating of Allende inclusions: Antiquity and fine structure. *Earth Planet Sci Lett* 47:211–222.
18. Hohenberg CM, Pravdivtseva OV, Meshik AP (2004) Trapped Xe and I-Xe ages in aqueously altered CV3 meteorites. *Geochim Cosmochim Acta* 68:4745–4763.
19. Blum JD, Wasserburg GJ, Hutcheon ID, Stolper EM (1989) Origin of opaque assemblages in C3V meteorites: Implications for nebular and planetary processes. *Geochim Cosmochim Acta* 53:543–556.
20. Urey HC (1956) Diamonds, meteorites, and the origin of the solar system. *Astrophys J* 124:623–637.
21. Urey HC (1959) Primary and secondary objects. *J Geophys Res* 64:1721–1737.
22. Clayton RN, Mayeda TK (1996) Oxygen isotope studies of achondrites. *Geochim Cosmochim Acta* 60:1999–2017.
23. Trieloff M, et al. (2003) Structure and thermal history of the H-chondrite parent asteroid revealed by thermochronometry. *Nature* 422:502–506.
24. Funaki M (2005) Natural remanent magnetization of chondrites and the magnetic field of protoplanets. *J Magn Soc Jpn* 29:918–925.
25. Nagata T (1979) Meteorite magnetism and the early solar system magnetic field. *Phys Earth Planet Inter* 20:324–341.
26. Sugiura N, Strangway DW (1988) *Meteorites and the Early Solar System*, eds JF Kerridge and MS Mathews (University of Arizona Press, Tucson, AZ), pp 595–615.
27. Hood LL, Cisowski CS (1983) Paleomagnetism of the Moon and meteorites. *Rev Geophys Space Phys* 21:676–684.
28. Banerjee SK, Hargraves RB (1972) Natural remanent magnetizations of carbonaceous chondrites and magnetic fields in early solar system. *Earth Planet Sci Lett* 17:110–119.
29. Sugiura N, Lanoix M, Strangway DW (1979) Magnetic fields of the solar nebula as recorded in chondrules from the Allende meteorite. *Phys Earth Planet Inter* 20:342–349.
30. Russell SS, et al. (2006) *Meteorites and the Early Solar System II*, eds DS Lauretta and HY McSween (University of Arizona Press, Tucson, AZ), pp 233–251.
31. Hood LL, Artemieva NA (2008) Antipodal effects of lunar basin-forming impacts: Initial 3D simulations and comparisons with observations. *Icarus* 193:485–502.
32. Wilson L, et al. (1999) Early aqueous alteration, explosive disruption, and reprocessing of asteroids. *Meteorit Planet Sci* 34:541–557.
33. Kleine T, et al. (2005) Early core formation in asteroids and late accretion of chondrite parent bodies: Evidence from ^{182}Hf-^{182}W in CAIs, metal-rich chondrites, and iron meteorites. *Geochim Cosmochim Acta* 69:5805–5818.
34. Greenwood RC, Franchi IA, Kearsley AT, Alard O (2010) The relationship between CK and CV chondrites. *Geochim Cosmochim Acta* 74:1684–1705.
35. Jogo K, Nakamura T (2009) A metamorphosed olivine-rich aggregate in the CV3 carbonaceous chondrite Y-86009. *72nd Annual Meteoritical Society Meeting* (Meteoritical Society, Tucson, AZ) p 5188.
36. Irving AJ, et al. (2004) A primitive achondrite with oxygen isotopic affinities to CV chondrites: Implications for differentiation and size of the CV parent body. *Eos Trans Am Geophys Union* 85(Suppl):P31C-02.
37. Meibom A, Clark BE (1999) Evidence for the insignificance of ordinary chondritic material in the asteroid belt. *Meteorit Planet Sci* 34:7–24.
38. Mothe-Diniz T, Carvano JM, Bus SJ, Burbine TH (2008) Mineralogical analysis of the Eos family from near-infrared spectra. *Icarus* 195:277–294.

GEOPHYSICS